Penerbit Akademia Baru

Malaysian Journal on Composite Science and Manufacturing

Journal homepage:
https://www.akademiabaru.com/submit/index.php/mjcsm/
ISSN: 2716-6945

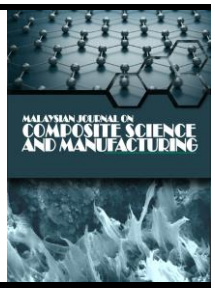

Electrical Conductivity and Antenna Properties of Polyaniline filled GNPs Nanocomposites

Open Access

Jeefferie Abd Razak[1], Nor Aisah Khalid[1], Hazman Hasib[1], Mazlin Aida Mahamood[1], Mohd Muzafar Ismail[2], Noraiham Mohamad[1], Poppy Puspitasari[3], Moayad Husein Flaifel[4,5]

[1] Fakulti Kejuruteraan Pembuatan, Universiti Teknikal Malaysia Melaka, Hang Tuah Jaya, 76100 Durian Tunggal, Melaka, Malaysia
[2] Fakulti Teknologi Kejuruteraan Elektrik & Elektronik, Universiti Teknikal Malaysia Melaka, Hang Tuah Jaya, 76100 Durian Tunggal, Melaka, Malaysia
[3] Mechanical Engineering Department, Fakultas Teknik, Universitas Negeri Malang, Jl. Semarang, No. 5, Malang, 65145, Jawa Timur, Indonesia
[4] Department of Physics, College of Science, Imam Abdulrahman Bin Faisal University, P.O. Box 1982, 31441, Dammam, Saudi Arabia
[5] Basic & Applied Scientific Research Center, College of Science, Imam Abdulrahman Bin Faisal University, P.O. Box 1982, 31441, Dammam, Saudi Arabia

ARTICLE INFO

Article history:
Received 15 September 2020
Received in revised form 7 January 2021
Accepted 07 January 2021
Available online 30 March 2021

ABSTRACT

This study was conducted to investigate the potential of utilizing conductive polymer nanocomposite for flexible type antenna application. The polyaniline (PANI) filled with graphene nanoplatelets (GNPs) nanocomposites were synthesized by an oxidative aniline polymerization in an acidic medium. The PANI/GNPs nanocomposites were then characterized by using various spectroscopy and imaging tools. It was found that the strong interaction between PANI macromolecules and GNPs flakes is caused by the strong π-π conjugation between them, as validated by an increase of I_d/I_g ratio of PANI/GNPs nanocomposites. As a result, it established a three-fold improvement for the electrical conductivity of PANI/GNPs nanocomposites, due to the larger amount of charge carrier transport at higher GNPs nanofiller loadings (1.00 wt.%). Later, the PANI/GNPs nanocomposites powder was applied to the cotton fabric by integrating it with a rubber paint slurry. Electrical conductivity, antenna gain, return loss, and radiation pattern of the antenna were reported. It was found that PANI/GNPs flexible textile antenna possessed a constant gain of 4.1809 dB, return loss at -13.154 dB, and radiation pattern which operated at 10.36 GHz for 100% improvement of electrical conductivity, in comparison with unfilled PANI. From these findings, it can be said that the development of wearable textile antenna utilizing PANI/GNPs nanocomposites on the cotton fabric as flexible radiation patch, has great potential for wireless communication purposes.

Keywords:
PANI/GNPs, polyaniline, graphene nanoplatelets, radiation patch, wearable antenna, wireless telecommunication

* *Corresponding author.*
E-mail address: jeefferie@utem.edu.my (Jeefferie Abd Razak)

https://doi.org/10.37934/mjcsm.4.1.1127

1. Introduction

Wearable textile antenna research is expanding swiftly, especially for applications in mobile computing, tracking navigation, and community safety. Up till now, the development of functional materials for wearable antenna development has been progressed, continuously [1]. The architecture of a common wearable antenna is consisting of a conductive radiation patch and a dielectric substrate. Investigation on both important parts is kept unending for optimizing the wearable antenna performances.

Flexible antennas are designed by smart clothing textile materials. Characteristic of electrical and electromagnetic properties will be the major reason to design this antenna. It integrates cloth into the communication system. The main requirements of the wearable antenna are lightweight, low cost, and easy installation requirements [2]. For wearable and flexible antenna application, it requires lightweight, small size, and low-profile antenna, which must show stable electrical properties, reasonable impedance resistance, and low energy consumption at desired radiation [3].

Previously, the conductive radiation patch for the antenna was merely fabricated from a copper sheet. However, copper metallic are uncompromising, costly, bulky, environmentally sensitive toward oxidation, and inflexible to manufacture. For wearable antenna on textile-based surfaces, it requires flexibility, durability, and conductive materials alternative, to be used as radiation patch replacement for copper [1]. Due to the limitation of copper metallic, carbon-based nanomaterials or conductive polymers are suitable options for further consideration. Examples of carbon nanomaterials are likes carbon nanotubes and graphene nanoplatelets, while the example of conductive polymers including polypyrrole, polyaniline, and many more. The remarkable electrical conductivity and flexibility of graphene nanomaterials have allowed them to be utilized as a potential candidate to replace uncompromising copper metallic.

This study was conducted to evaluate the potential of a new formulation of polyaniline conductive polymer filled with graphene nanoplatelets (PANI/GNPs), for flexible wearable textile antenna application. In this study, the PANI/GNPs nanocomposites powder was synthesized by aniline polymerization in an acidic medium. Later, it was integrated with the rubber slurry, prior to thin coating to the cotton fabric. The effects of GNPs nanofiller loading on the antenna radiating properties for GNP/PANI-textile nanocomposites were characterized by using standard physical, electrical, and general antenna characterization methods [3].

PANI polymer exists in a variety of forms, which differ in their chemical and physical properties. The most common green protonated emeraldine has conductivity on a semiconductor level of the order of 10^0 S cm^{-1}, but lower than any of typical metals (>10^4 S cm^{-1}). On a commercial basis, PANI shows a great promising future for various product applications. They can replace metals and semiconductors, as they have acceptable conductivity, lower density, and easy manufacturability. Simple synthesis and high environmental stability attributes made PANI becoming more versatile in their polymer family. PANI and its subordinates are being utilized in innovative applications due to reversible proton doping, higher electrical conductivity, and simplicity of mass fabrication [5]. Modification of PANI through composite strategy had previously investigated, such as on the development of microstrip antenna segment from PANI based textile, that can increase the usage of wireless devices [6, 7], while the development of electron storage through in-situ polymerization of TiO_2-TVC/PANI composite film had increased the electron storage into a maximum of 3689.3 C/mol [8]. In this study, PANI was utilized as an electro-conductive polymeric-based matrix for functional type nanocomposite development.

To further enhance the electrical conductivity of PANI, it was intrigued to incorporate them with conductive nanofiller like carbon-based nanomaterials. One of the promising candidates was GNPs. Graphene is described as two-dimensional (2D) nanomaterials that possessed higher electrical conductivity, good thermal and chemical stability, outstanding mechanical strength, extraordinary optical behavior, and a large surface-to-volume ratio than carbon nanotubes (CNTs) [9]. The electrical conductivity of GNPs parallel to the surface is 10^7 S/m while perpendicular to the surface is about 10^2 S/m [10]. Besides, the planar structure of GNPs provides a 2D pathway for phonon transport for efficient thermal conductivity of about 3000 – 5000 W/m.K [10]. Graphene has lower costs and easy to synthesize in the bulk form [11]. GNPs are graphite nanocrystals corresponding to the platelets which contain multiple layers of graphene. GNPs can be utilized to reinforce the properties of various polymeric materials.

In this work, GNPs were integrated with PANI at various loadings and later followed by integrating it with rubber slurry for conductive paste preparation. The role of GNPs in the development of a conductive radiating patch for wearable antenna application, based on the tested properties of produced PANI/GNPs nanocomposites were evaluated. The combination of GNPs and PANI has complementing each other, to enhance the electrical conductivity properties [12]. It was expected that the antenna made from PANI/GNPs-textile nanocomposites could be beneficial as smart clothing for wearable antenna fabrication, which feasible for wireless communication technology.

2. Methodology

2.1 Synthesis of PANI/GNPs Nanocomposites Powder and Conductive Rubber Slurry Preparation

For pristine PANI preparation, about 22.84 grams of ammonium peroxydisulfate (APS) and 10.36 grams of aniline hydroxide were separately dissolved in 200 ml of distilled water. Later, the pre-cooled step was followed for both solutions at 282K for 12 hours. Then, the precooled solutions were mixed in a beaker and stirred for one hour by using a magnetic stirrer. The stirred and mixed solution was left in a chiller at 282K for 24 hours. The precipitated powder was then filtered by using a vacuum filter at 50 kPa. While the filtering process was performing, the mixture has been washed with 200 ml of 0.20 M of hydrochloric acid and 200 ml of acetone. Finally, the drying of the filtered powder mixture was performed in a vacuum oven for 24 hrs at 60°C.

For the synthesis of PANI/GNPs nanocomposites at different loadings of GNPs (0.25, 0.50, 0.75, and 1.00 wt.%), the GNPs content was based on 100 % of APS and aniline hydrochloride total weight basis. The respective GNPs weight amount has been added after the first pre-cooled step, during the solution mixing at one hour, before it being left to cool again at 9°C for 24 hrs. The subsequent following steps are similar to the preparation of pristine PANI until the nanocomposite powder of PANI/GNPs has been completely prepared.

For integration between PANI/GNPs nanocomposites powder with the rubber slurry, the standard commercial rubber slurry of silk printing grade was purchased and used as is together with the added PANI/GNPs at each respective formulation. The conductive rubber paste was then applied to the cotton fabric as a thin coat and let cure under room temperature. The coating dimensional was on top of the cotton fabric, was following the geometrical dimension of the produced antenna as available in the following Table 1.

2.2 Structural, Physical, Chemical and Morphological Characterization of Pristine PANI and PANI/GNPs Nanocomposites Powder

For characterization, unfilled pristine PANI is used as a control sample for the entire related testing. In this study, the effect of GNPs loading on the crystallinity and morphological structure of PANI/GNPs nanocomposites was evaluated by X-ray diffraction (XRD) analysis. For this characterization, it was carried out by using PanAnalytical diffractometer model X'PERT PRO MPD PW3060/60 which operated at 40 kV and 30 mA, using Cu Kα radiation with λ = 0.154 nm of wavelength. The scans were taken in between 10 - 80° range at a scan rate of 0.05° per second with a continuous scan step size of 0.0170°.

For chemical-related analysis, a Fourier Transform Infra-Red (FTIR) spectroscopy model JASCO FT/IR-6000 was utilized to confirm the presence of functional group and to differentiate the structure between the unfilled pristine PANI as a control sample with the PANI/GNPs nanocomposites. The attenuated total reflectance ATR-FTIR analysis was conducted at 25°C, at a resolution of 4.00 cm^{-1} and between the wavenumber ranges of 500 to 1800 cm^{-1}, by using a scan rate of 2.00 mm/s with an aperture size of 7. 10 mm.

Raman spectrometer analysis was performed to analyze the structural properties of PANI and PANI/GNPs nanocomposites. The analysis was conducted by using UniRAM-3500 set-up with an argon-ion laser at < 0.02 mW and 514.5 nm excitation within the experimental range in between 900 – 1900 cm^{-1}.

DC-conductivity measurement by using a four-point probe method was conducted to measure the electrical conductivity value of pristine PANI and PANI/GNPs nanocomposites samples. The test was conducted in accordance with the ASTM D999-89 standard. A four-point probe machine model Jandel RM3-AR In-Line test equipment was utilized in this study. Sample of PANI and PANI/GNPs nanocomposites were pressed into the pallet form having a dimension of 2.80 mm thickness and 9.00 mm diameter by using a hydraulic press machine, at room temperature setting.

For morphological observation of produced pristine PANI and PANI/GNPs nanocomposites powder samples, it was performed by using the scanning electron microscope (SEM) model Zeiss EVO50. The observations on the selected samples (pristine PANI as the controlled sample, PANI/0.25 wt.% GNPs, PANI/0.75 wt.% GNPs, and PANI/1.00 wt.% GNPs) nanocomposites were performed at the magnification of 1000x under the accelerating voltage of 15 kV. All samples were coated with gold-palladium coating using a sputter coater model Polaron prior to the imaging, to prevent the electrostatic charging phenomena.

2.3 Antenna Fabrication and Antenna Performance Characterization

For wearable antenna design, it was first simulated by using the CST software. Single-layer wearable antenna design has consisted of two major components which are the flexible substrate (in this case, the cotton fabric) and the flexible conductive patch (in this case, the pristine PANI or PANI/GNPs nanocomposites rubber slurry). The proposed antenna structure based on simulation was depicted as in Figure 1. Also, about 20 mm of conductive tape was used to connect the SMA port to VNA female low lost test cable. Overall, the substrate dimension was 20 mm x 20 mm, while the cotton fabric used has a dimension of 23 mm x 23 mm. The geometrical specification of the fabricated wearable antenna made from PANI/GNPs rubber slurry nanocomposites on top of cotton fabric was summarized in Table 1.

The electrical conductivity of the antenna made from PANI/GNPs nanocomposites rubber slurry was measured by using a four-point probe brand Jandel model RM3-AR probe, with a measuring range between 10^{-12} to 10^{0} S/m.

For antenna performance, the microstrip antenna patch was attached to the SMA connector. Antenna parameters such as the return loss, radiation pattern, and radiation gain were then tested. Return loss is to determine the antenna matching properties and it was measured by using the variable network analyzer, VNA (HP Agilent 8722ES, Santa Clara, CA, USA). The textile integrated antenna was connected to an SMA connector and a 50 Ω co-axial cable was used to connect the VNA and the SMA connector. VNA contains both transmission and reflection sources and is used to generate known stimulus caused by device-under-test (DUT). The stimulus is injected into the DUT and VNA measure both signals that are being reflected from the input side, as well as the signal passing through the DUT output side [13]. The VNA receiver measured the resulting signal and compared it to the known stimulus signal. Measured results are then processed either by an external PC and sent to display for further analysis.

Table 1
Dimensional details of produced PANI/GNPs wearable antenna

Features	Dimension
Substrate height	1.50 mm
Substrate width	20.00 mm
Substrate length	20.00 mm
Cotton fabric width	23.00 mm
Cotton fabric length	23.00 mm
Conductive tape length	20.00 mm

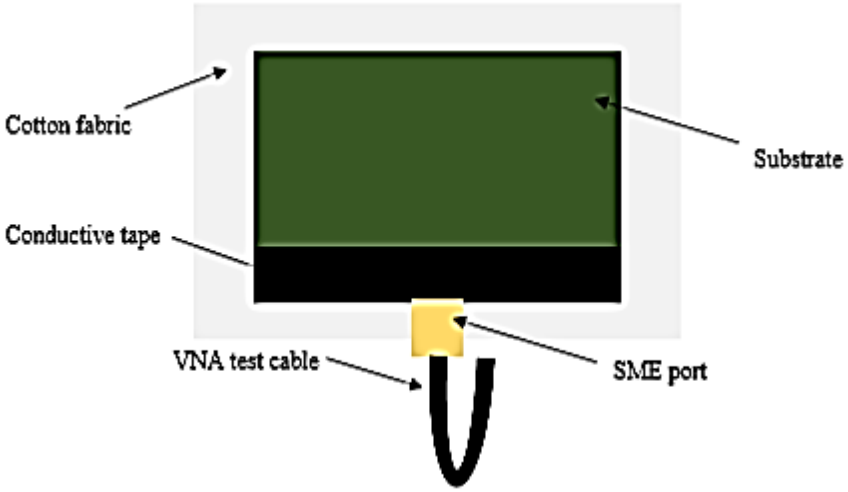

Fig. 1. The design structure of a single-layer wearable textile antenna

3. Results

3.1 X-Ray Diffraction (XRD) Analysis of PANI/GNPs Nanocomposites Powder

Figure 2 shows the characteristics of X-ray diffraction patterns of pristine PANI and PANI/GNPs nanocomposites at various GNPs loadings. Pristine PANI shows a broad and diffused peak at 2θ = 21° which indicates the crystallinity behavior of produced PANI. Several important peaks for pristine PANI

at 2θ = 15°, 21°, and 26° are corresponded to 011, 020, and 200 diffraction planes, respectively. By adding the GNPs nanofiller at 0.25, 0.50, 0.75, and 1.00 wt.% of loadings, it has increased the intensity at 2θ = 26° which corresponded to the intense crystallinity of graphene. This situation has suggested the strong interaction between the PANI macromolecular backbones with the GNPs nanofiller. Besides, this also suggests the homogeneous dispersion of GNPs within or in-between PANI polymer macromolecules [12].

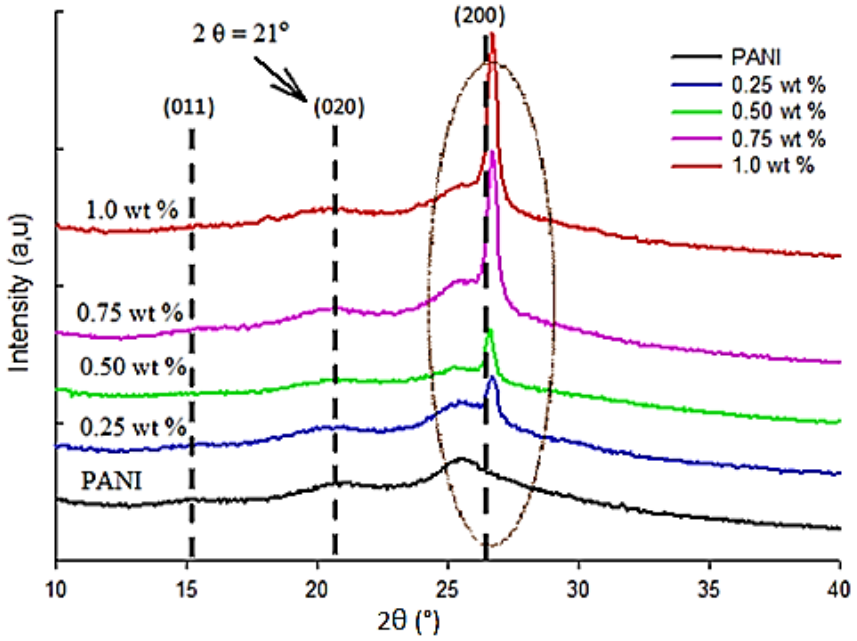

Fig. 2. X-Ray Diffraction (XRD) pattern of pristine PANI and PANI/GNPs nanocomposites

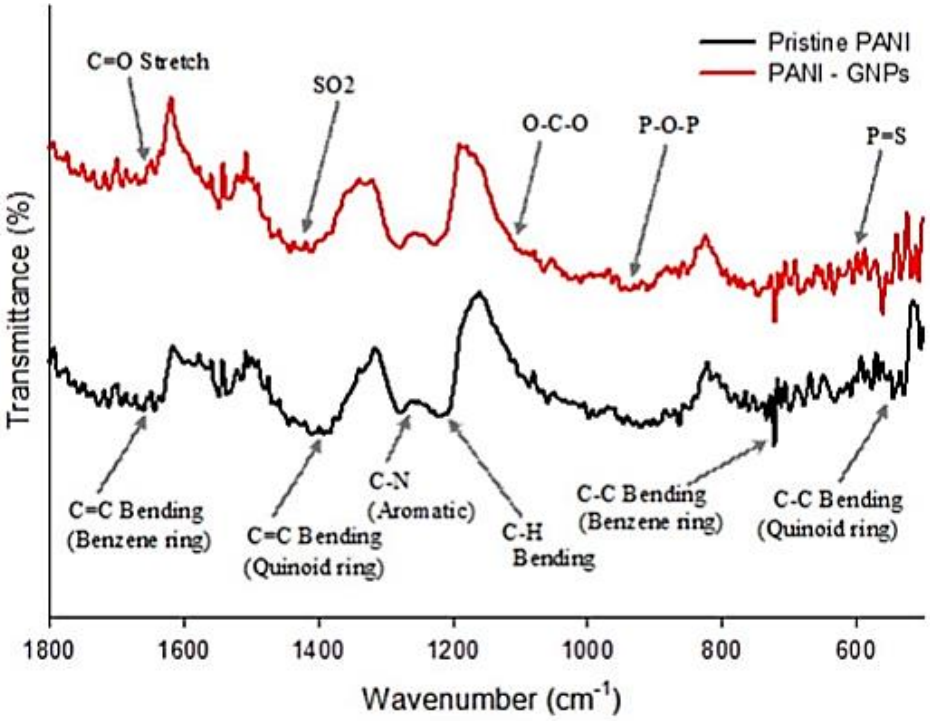

Fig. 3. FTIR spectra of pristine PANI and PANI/GNPs nanocomposites

3.2 Fourier Transform Infra-Red (FTIR) Analysis of PANI and PANI/GNPs Nanocomposites

The presence of functional groups in pristine PANI and PANI/GNPs nanocomposites was evaluated by using FTIR spectra, as depicted in Figure 3. Pristine PANI as shown as black color spectra, the vibrational peaks at 1600 and 1400 cm^{-1} were the characteristic of C=C bending conjugated in quinoid and benzoid ring vibration, respectively [11]. In addition, an absorption peak at 1200 cm^{-1} was corresponded to C-H in-plane bending, while both peaks at 700 and 530 cm^{-1} correspond to C-C bending from benzene and quinoid rings, respectively [12]. For PANI/GNPs nanocomposite sample, the FTIR curve shows an obvious peak at 1412.9 cm^{-1} that corresponds to the sulphur dioxide group which refers to the interaction between PANI and GNPs during the in-situ polymerization. The absorption peak at 974.41 cm^{-1} shows the formation of covalent phosphorus. The PANI/GNPs nanocomposite has retained the entire major characteristic peaks of pristine PANI with the significant increase in their intensity, that suggesting the establishment of weak Van der Waals interaction between the PANI backbone and GNPs nanofiller in the resulted PANI/GNPs nanocomposite [14, 15].

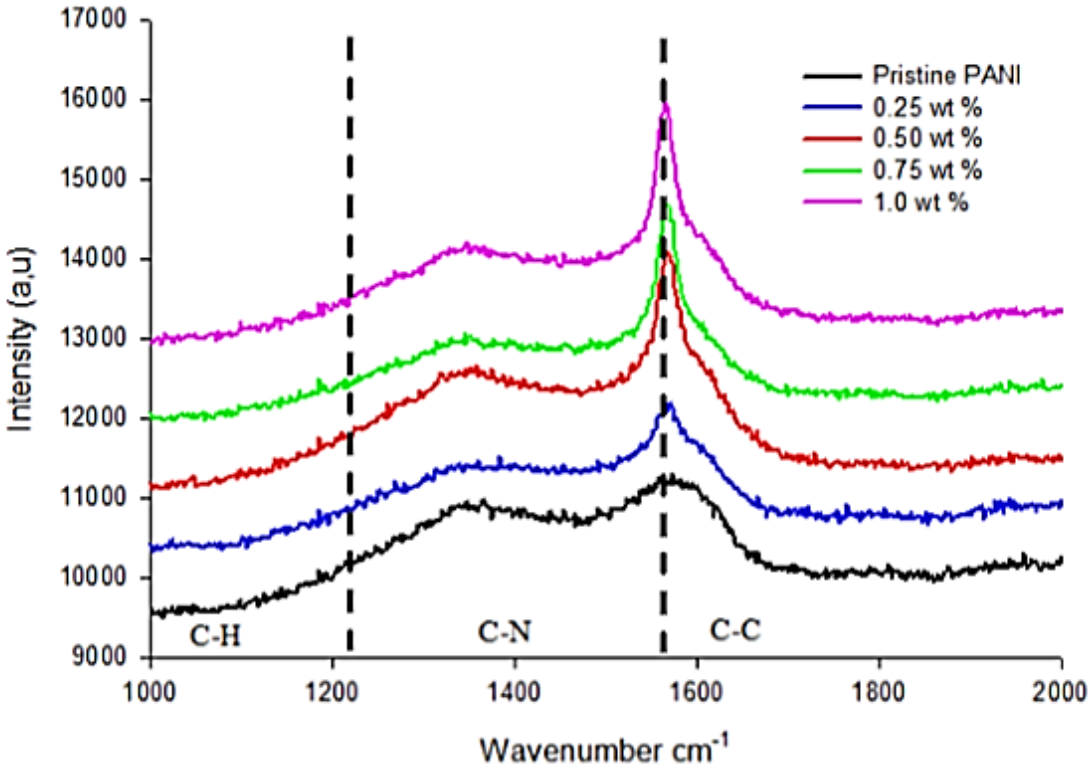

Fig. 4. Raman spectra of pristine PANI and PANI/GNPs nanocomposites

3.3 Raman Spectroscopy Analysis of Pristine PANI and PANI/GNPs Nanocomposites

In this study, Raman spectroscopy analysis was performed to evaluate the information on PANI/GNPs physico-chemical structure. Raman spectra of pristine PANI and PANI/GNPs nanocomposites with different GNPs loadings are depicted in Figure 4. Basically, for PANI based

samples, there is three important vibrational range, which is C-H bending mode at between 1100 – 1210 cm^{-1}, several C-N stretching modes (polaron, imines, and amines) at between of 1210 – 1520 cm^{-1} and C-C stretching modes at between of 1520 cm^{-1} that attribute to benzoid C-C stretching mode, into 1650 cm^{-1} which attributed to quinoid C-C stretching mode. These Raman spectra also represent two strong bands corresponds to the D and G band at 1300 cm^{-1} and 1600 cm^{-1}, respectively. A strong π-π electron conjugation between the PANI backbone and GNPs phases has been confirmed by an increase of I_d/I_g ratio of PANI/GNPs nanocomposites with the increase of GNPs loadings [12, 13].

3.4 Four Point Probe DC-Electro Conductivity of PANI and PANI/GNPs Nanocomposites

Electrical conductivity performance of pristine PANI as the control sample and PANI/GNPs nanocomposites with various loading of GNPs filler was explained based on sheet resistance measurement. The PANI-based powder was first pressed by using a compaction method to prepare a disc-shaped pellet with a thickness of less than 3.00 mm. PANI electric conductivity is caused by conjugation in the polyaniline backbone, where PANI has both benzoid and quinoid units. The polar and bi-polar movement along the polymer backbone has responsibly caused the polymer electro-conductivity mechanism [16].

Figure 5 depicts the DC conductivity plots of pristine PANI and PANI/GNPs nanocomposites, measured by the four-point probe method. Based on the plots, it was found that at lower content of GNPs (0.25 wt.%) lower conductivity value has been generated as compared to the conductivity of pristine PANI. It is due to the lower concentration of GNPs that disrupted the PANI macromolecular backbone. Therefore, the lower GNPs loadings have prevented the formation of complete micelle when the aniline polymerization was taking place.

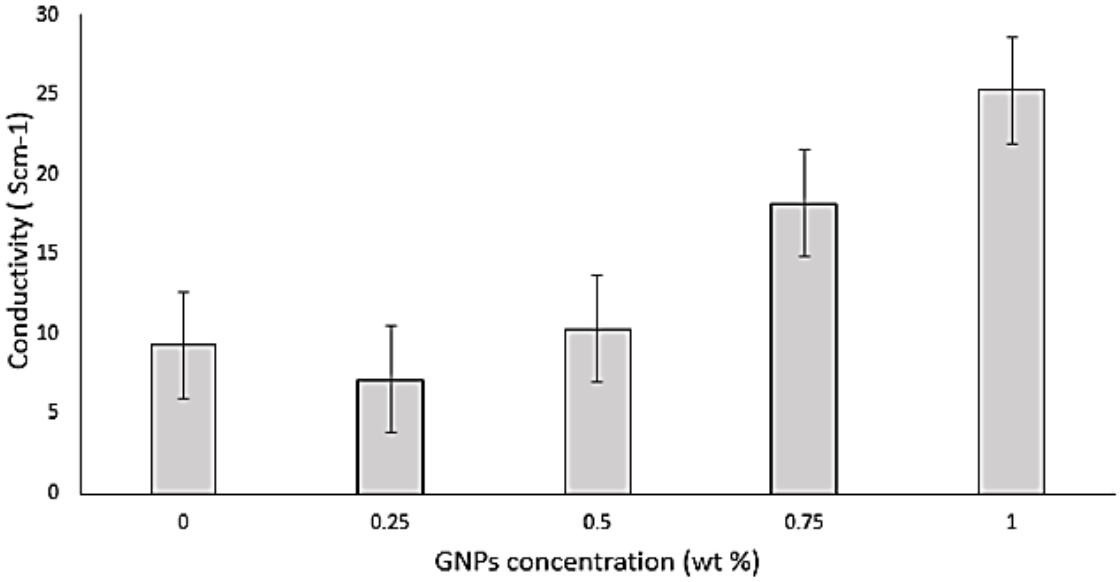

Fig. 5. DC-Conductivity plots of pristine PANI and PANI/GNPs nanocomposites

However, the conductivity values have proportionally increased with the increase of GNPs content, especially at higher filler loading. The presence of GNPs at higher loading helps to promote

the polymerization by stabilizing and increasing the PANI micelles size, which induced uninterrupted polymerized conditions that increase the conductivity. In addition, good contact between GNPs flakes also promotes the current transport due to less resistance between platelet which interlinked between each other to establish the alternative current network path for better electrical conductivity [17].

3.5 Scanning Electron Microscope (SEM) Observation of PANI and PANI/GNPs Nanocomposites

SEM observation was performed to observe the morphological characteristic of pristine PANI and PANI/GNPs nanocomposites at various GNPs filler loading (Figure 6). Pristine PANI as the controlled sample, while PANI/GNPs nanocomposites at 0.25 and 0.75 wt.% are selected to represent filled PANI at lower GNPs addition and PANI/1.00 wt.% GNPs for nanocomposites at higher GNPs loading, for comparison.

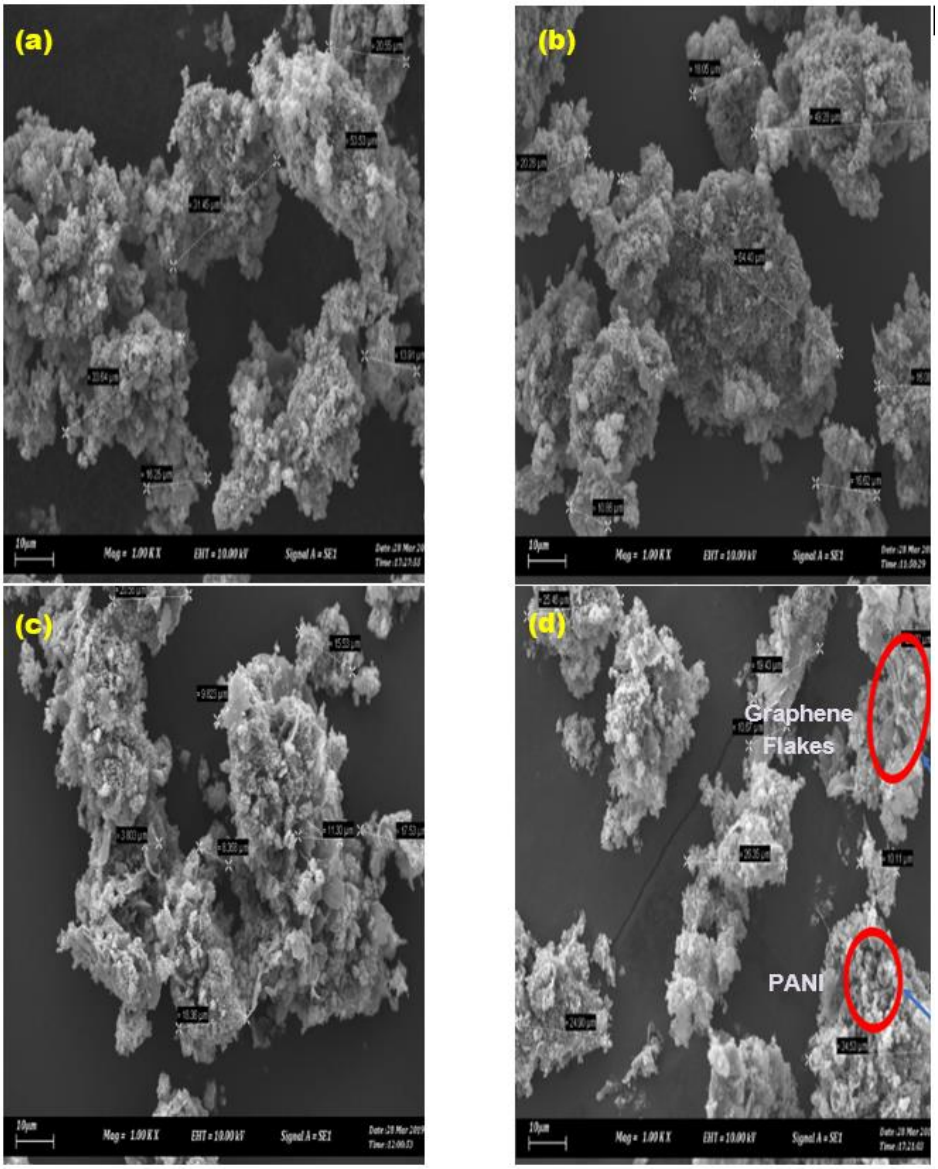

Fig. 6. SEM images of pristine PANI and PANI/GNPs nanocomposite (1000x of magnification); (a) pristine PANI; (b) PANI/0.25 wt.% GNPs; (c) PANI/0.75 wt.% GNPs; and (d) PANI/1.00 wt.% GNPs

Pristine PANI as depicted in Figure 6a possessed agglomerated globular shape. However, the morphology of PANI globular has been significantly changed after the presence of GNPs in PANI/GNPs nanocomposites for all loading percentages. At 0.25 wt.% of GNPs addition, the presence of graphene flakes has destructed the agglomerates globular of PANI polymer (Figure 6b). At lower filler loading, better dispersion of GNPs within PANI has separated the macromolecules and prevent the formation of the agglomerate. This situation had caused a reduction in PANI globular sizes. It also explained the significant reduction of DC conductivity value in comparison to pristine PANI sample, due to the destruction between PANI macromolecules interlinkage chains.

However, by increasing further the GNPs loading of more than 0.25 wt.%, it was found that good integration between GNPs nanofiller and PANI macromolecules cluster was established, due to successful in-situ oxidative aniline polymerization reaction which further dispersed the GNPs nanofiller (Figure 6c). Flaky morphology with several flat and edges surfaces can be detected throughout the PANI cluster, which indicating better dispersion of GNPs. It proved that the aniline monomers were diffused and polymerized into graphene nano-sheets layer by layer during in situ polymerization [18].

At higher loadings (1.00 wt.%) of GNPs, the SEM micrograph of PANI/GNPs nanocomposite (Figure 6d) also revealed that the GNPs were homogeneously distributed within the PANI matrix. The presence of GNPs within the PANI matrix has led to enhance the electro-conductivity characteristic of PANI/GNPs nanocomposites as proven in this study. The presence of GNPs has successfully given the alternative pathway for current movement, due to network inter-linkage between the graphene platelets together with PANI macromolecules clusters [19].

3.6 Design and Simulation of Wearable Antenna using CST Microwave Studio and Antenna Experimental Performances Results for PANI/GNPs based Nanocomposites on Cotton Fabric

Prior to wearable antenna fabrication, it was first simulated by using the Computer Simulation Technology (CST) Microwave Studio. The simulation results were then compared with the experimental results using a similar antenna design as simulated by the CST software (Figure 7). The proposed wearable textile antenna was simulated in an antenna simulation software to produce very sharp antenna attributes such as return loss, gain, and radiation pattern of the antenna.

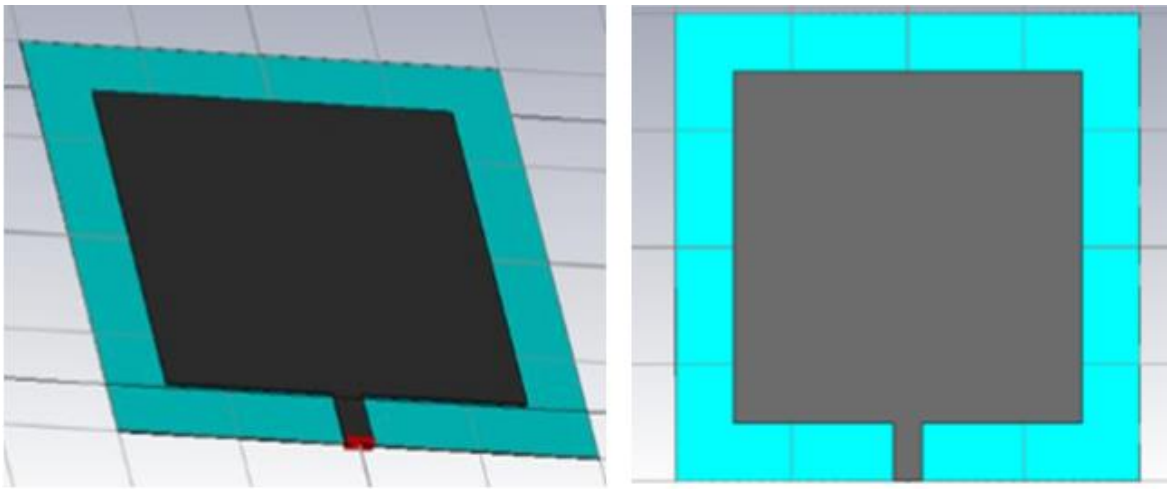

Fig. 7. Side and view images of simulated antenna microstrip patch

For simulation, the minimum frequency was set to 1 GHz and maximum at 5 GHz. Figure 7 depicts the antenna image designed by the CST microwave studio. A square patch antenna was designed into 20 mm x 20 mm of a cotton dielectric substrate and 18 mm x 18 mm of conductive radiation square patch. Table 2 summarized the overall dimension of simulated antenna design.

Figure 8 depicts the simulated return loss plots. It was shown that the return loss was achieved at -13.154 dB at 3.40 GHz frequency. This indicates a good sign for the antenna to be operated efficiently, at least at -10.00 dB. The operating frequency at 3.40 GHz indicates that the produced PANI/GNPs antenna could perform at a short-range communication system. By adjusting the patch dimension, the return loss values were changed accordingly.

Figure 9 depicts the experimental return loss results for PANI/GNPs based wearable antenna at difference GNPs loadings and unfilled pristine PANI as the control sample. The return loss results are from the VNA analyzer. The return loss plots were increased with the increase of GNPs loadings. Patch antenna of PANI with 1.00 wt.% GNPs loading had generated a similar return loss value of -13.154 dB at the 10.36 GHz operating frequency, with the simulated design which differs at 3.80 GHz of the operating frequency. The difference may due to the fabrication factor and for the simulated result, only graphene data were taken into consideration while for the experimental, both combinations of PANI and GNPs need to be considered. Overall, the higher the GNPs loading, the bigger the return loss concentration peak.

Table 2
The overall dimension of simulated antenna design

Component	Part	Dimension (mm)
Cotton Substrate	Length	20.00
	Width	20.00
	Thickness	0.85
Radiation Patch	Length	18.00
	Width	18.00
	Thickness	0.04
Feed Line	Length	2.00
	Width	2.40

Antenna gain of PANI/GNPs based microstrip was measured by using a VNA analyzer. Antenna gain (G) can be defined as the proportion of power density at the maximum radiation direction at an equal distance above the isotropic antenna when transmitting the equal power. It was expressed in the dB unit. The antenna gain (G) value was calculated at 4.1809 dB for operating frequency at 10.36 GHz. With this gain value, it can be said that the antenna possessed good efficiency.

The antenna gain value was circled in Figures 10 (a) and (b). Proper antenna fabrication technique was prominent in affecting the efficiency value which was influenced by the conductivity value of radiating patch.

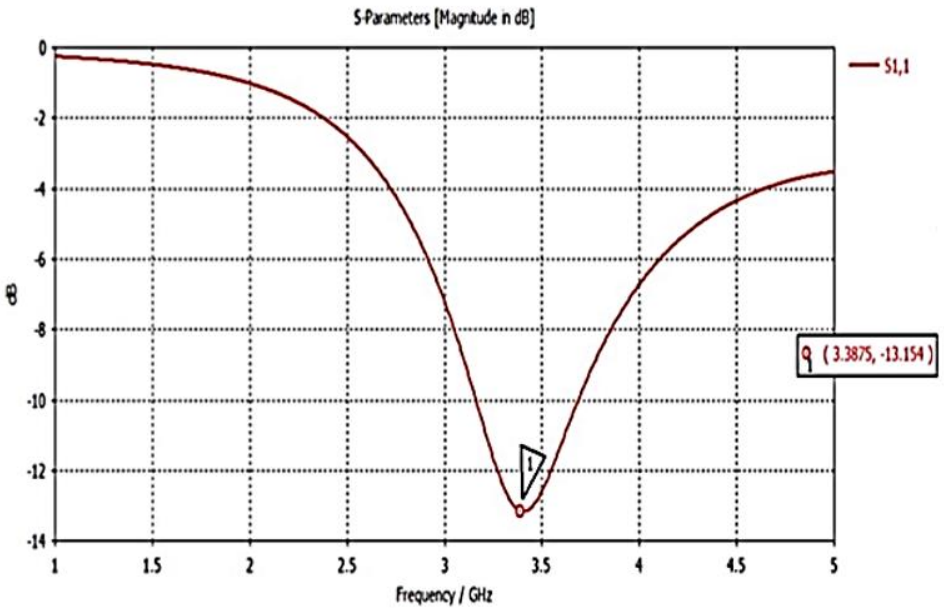

Fig. 8. Simulated return loss results for PANI/GNPs microstrip patch antenna design

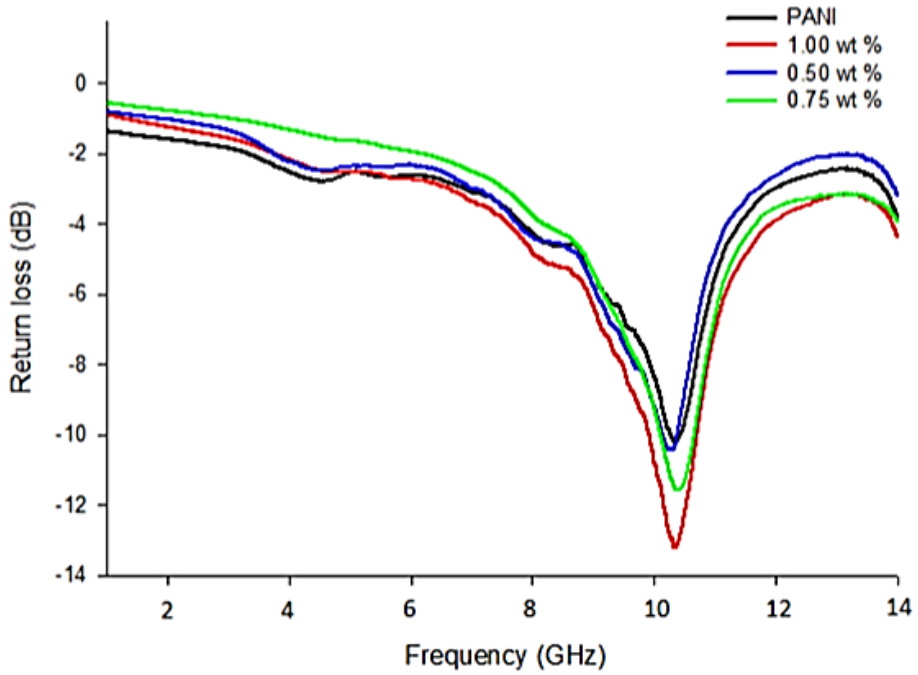

Fig. 9. The experimental return loss results of pristine PANI and PANI/GNPs based microstrip patch at various GNPs loadings

While the radiation pattern can be defined as relative emitted power distribution as a function of inner space [20, 21]. It was measured in an anechoic chamber by using the Aronia HyperLOG-7060 antenna and tuneable signal generator on the transmission side, while the textile sample was kept fixed on a dielectric holder and acted as a far-field receiver [13]. It is also defined as a field pattern; a plot of amplitude that is a magnetic field radiated by an antenna in a space coordinate. Power pattern can be defined as the square of magnetic field magnitude.

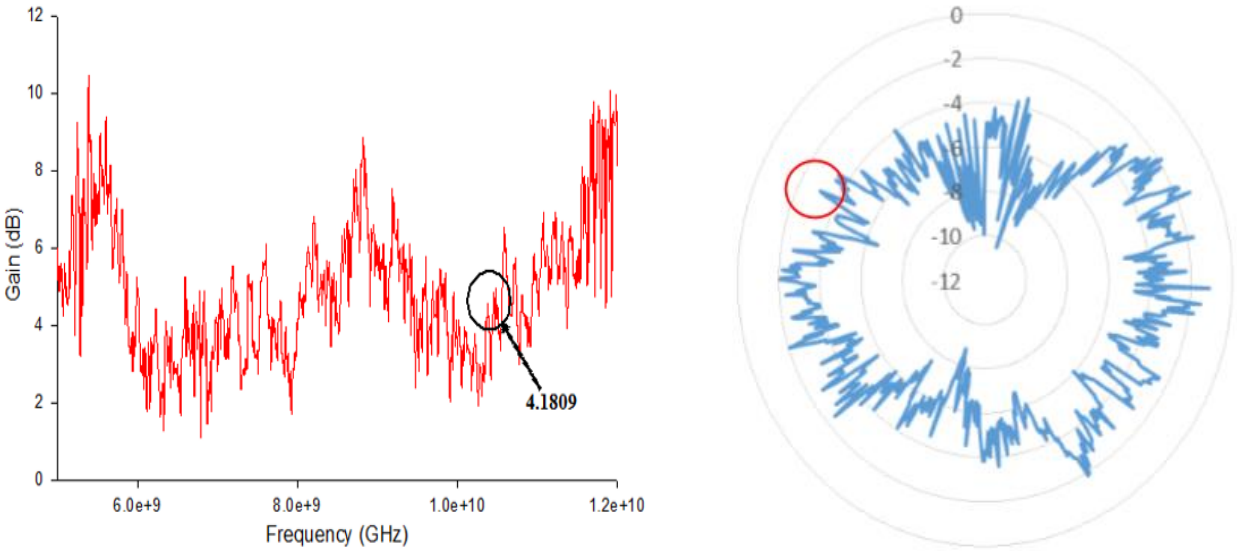

Fig. 10. (a) Antenna gain measured by VNA; (b) Antenna gain at 4.1809 dB at 10.36 GHz operating frequency

The radiation pattern of the simulated antenna design was depicted in Figure 11. This radiation pattern has resulted from the omnidirectional plot at the frequency of 10.36 GHz. The main lobe magnitude was at 6.12 dB and the main lobe direction was at 129.0°. In addition, the angular width at 3.00 dB was at 31.4°, with the side lobe level at -1.50 dB. Detail observation of the pattern has found that it was disturbed from an omnidirectional pattern to spread out at a frequency of 10.36 GHz, where the pattern becoming pure directional with its side lobe. This kind of pattern has allowed the antenna to be used where the directional antenna was needed in point-to-point communication with a station and with other members using the station as the base, which is a pure directional system [22].

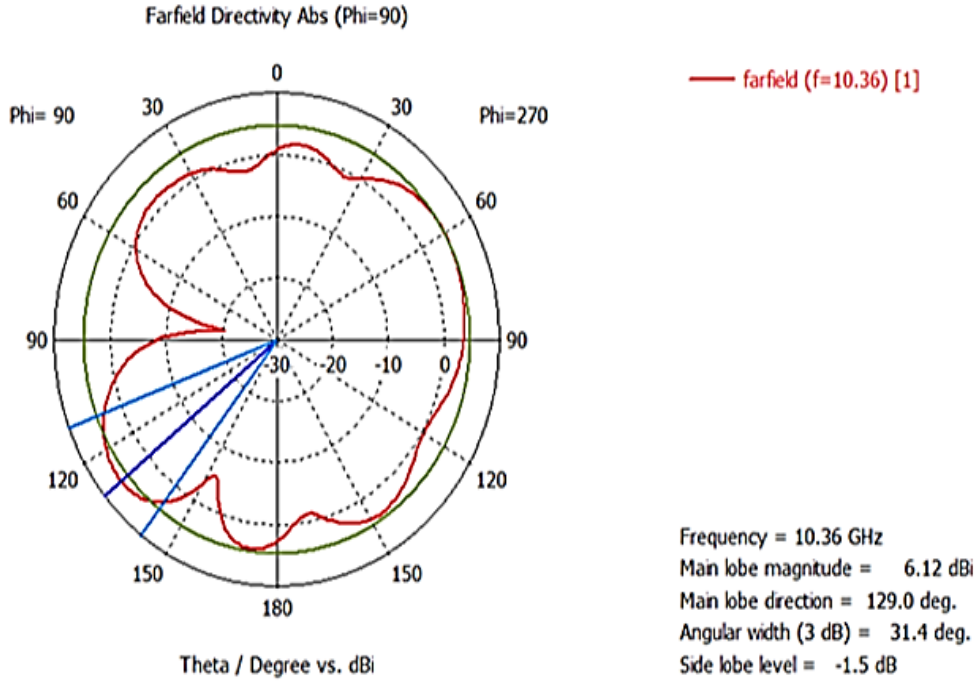

Fig. 11. The radiation pattern of the simulated antenna design

Figure 12 has presented a radiation pattern of PANI/GNPs type experimental antenna design. The radiation pattern shows an inequality pattern as compared to the simulated radiation pattern. This condition might be contributed by the GNPs dispersion state within the PANI conductive polymer matrix. The GNPs nanofiller dispersion has significantly influenced the conductivity value, due to the interconnection network that was established between the graphene platelets and PANI macromolecules, which facilitate further the electrical conductivity [23].

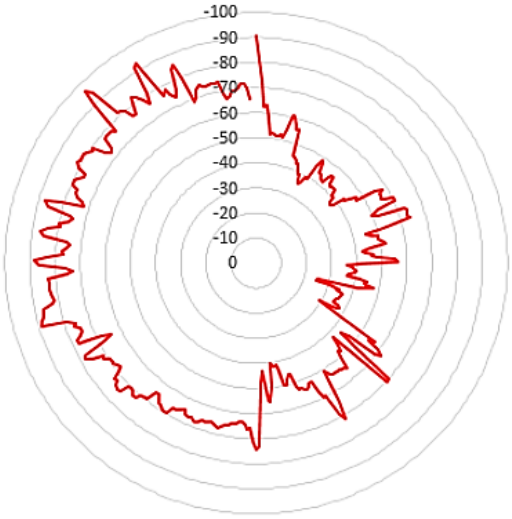

Fig. 12. The radiation pattern of the PANI/GNPs experimental antenna design

Electrical conductivity characteristics of PANI/GNPs nanocomposites at various GNPs loadings when integrated with cotton fabric as wearable antenna substrate were also evaluated.

Table 3 and Figure 13 has summarized the electrical conductivity values of each wearable textile antenna made up of unfilled PANI as control sample and PANI/GNPs nanocomposites at various GNPs loadings. It can be observed that the conductivity values were amplified with the increase of GNPs loadings.

This situation was following the electrical conductivity results for PANI/GNPs powder when it was tested using a four-point probe method prior to integration with the cotton substrate. The highest conductivity value was possessed by the PANI/GNPs nanocomposites with 1.00 wt.% of GNPs integrated onto the cotton fabric. Significance reduction of the conductivity value shown by PANI/GNPs on the antenna as compared to PANI/GNPs in the powder pallet form was due to the dielectric behavior of cotton fabric which functions as an insulating substrate. Moreover, the rubber pastes which function as a binder between the PANI/GNPs powder into substrate have diminished the conductive network established by the graphene platelets by introducing the barrier between the conductive nanofiller.

Hence, for future investigation, this limitation is needed to be resolved, to make sure the flexible conductive polymer substrate performs the function of the as efficient radiating patch at the highest performance possible, for better antenna characteristics. This is important as the antenna performances are proportional to the electrical conductivity state of the radiation patch component.

Table 3
Electrical conductivity data of wearable textile antenna with pristine PANI (control) and PANI/GNPs with various GNPs nanofiller loadings

GNPs concentration (wt.%)	Pristine PANI (unfilled)	0.25	0.50	0.75	1.00
Conductivity (Scm^{-1})	9.09	7.40	13.80	15.92	18.17

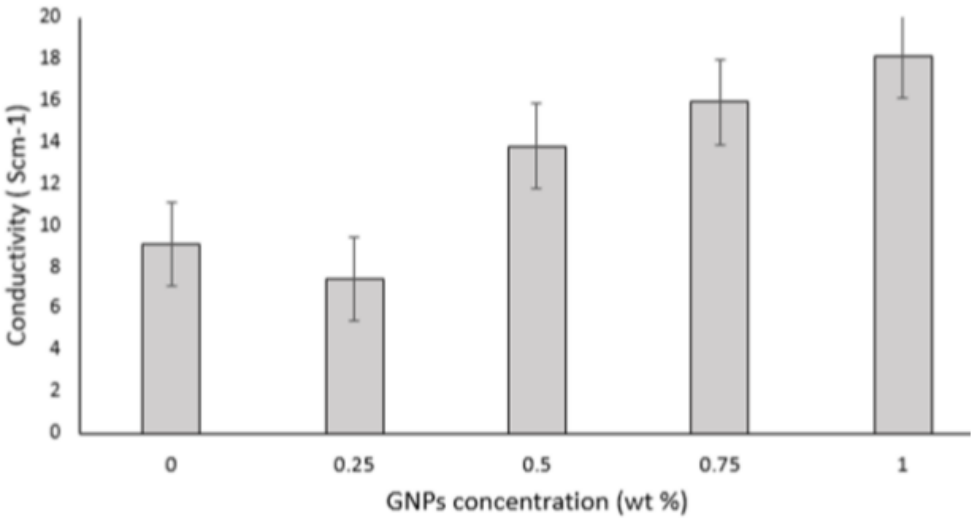

Fig. 13. Conductivity plots of the wearable textile antenna of pristine PANI and PANI/GNPs nanocomposites with various GNPs loadings

4. Conclusions

In this work, pristine PANI and PANI/GNPs nanocomposites with various loadings of GNPs have been successfully synthesized through an oxidative aniline in situ polymerization method. This has been confirmed by the output findings from Raman and FTIR spectroscopy analysis. The XRD and Raman findings again have confirmed the dispersion state and well-integration of GNPs within the PANI macromolecules. This has further been proven by the SEM micrograph which also explained the positive trend of DC conductivity results pattern, which was proportionally increased with the increase of GNPs loadings. Overall, the addition of GNPs into conductive PANI is potentially being able to further improve the electrical conductivity properties of pristine PANI and PANI/GNPs nanocomposites. The addition of 1.00 wt.% of GNPs into PANI/GNPs nanocomposites had contributed to 100% improvement of electrical conductivity, in comparison with unfilled PANI. This has certainly benefited various impending high-impact applications for future utilization. Moreover, in this study, the wearable textile antenna made from graphene-like material was simulated by the CST software. By comparing with experimental results, the wearable antenna made from PANI/GNPs nanocomposites as the radiating patch is feasible with promising constant gain at 4.1809 dB, return loss at -13.154 dB, and with acceptable antenna radiation pattern operated at 10.36 GHz.

Acknowledgment

Special acknowledgement to the Fakulti Kejuruteraan Pembuatan and Centre of Smart System and Innovative Design (COSSID), Universiti Teknikal Malaysia Melaka (UTeM) for providing all the facilities to complete this study. Special thanks to UTeM for providing the research funding under the short-term research grant: PJP/2019/FKP(4B)/S01662.

References

[1] A. Tsolis, W. G. Whittow, A. A. Alexandridis and J. C. Vardaxoglou, "Embroidary and Related Manufacturing Technique for Wearable Antennas: Challenge and Opportunities," Electronics 3, no. 2 (2014): 314-338. https://doi.org/10.3390/electronics3020314

[2] W. M. Hassan and A. M Attiya, "Textile Antenna Integrated with a Cap for Li GPS Application," (PDF, 35th National Radio Science Conference (NRSC), Cairo, March 20-22, 2018). https://doi.org/10.1109/NRSC.2018.8354357

[3] S.H. Dar and J. Ahmed, "Characterization of Flexible Wearable Antenna based on Rubber Substrate," International Journal of Advanced Computer Science and Applications 7, no. 11 (2016): 190-195. https://doi.org/10.14569/IJACSA.2016.071124

[4] S. Shahabuddin, N.M. Sarih, S. Mohamad and S.N.A. Baharin, "Co3O4 Nanocube-doped Polyaniline Nanocomposites with Enhanced Methyl Orange Adsorption from Aqueous Solution," RSC Advances 49, no. 6 (2016): 43388-43400. https://doi.org/10.1039/C6RA04757B

[5] H.S. Abdulla and A.I. Abbo, "Optical and Electrical Properties of Thin Films of Polyaniline and Polypyrole," International Journal of Electrochemical Science 7, (2012): 10666-10678. http://www.electrochemsci.org/papers/vol7/71110666.pdf

[6] A. Frederick, "Smart Nanotextiles: Inherently Conducting Polymers in Healthcare," de Vinci's Notebook 3, (2011): 1-2.

[7] A. Yadav, V. K. Singh, M. Chaudhary and H. Mohan, "A Review on Wearable Textile Antenna," Journal of Telecommunication, Switching Systems and Networks 2, no. 3 (2015): 37-41.

[8] W. Boonmeemak, C. Fongsamut and P. Ngaotrakanwiwat, "Development of TiO_2/TiO_2-V_2O_5 Compound with Polyaniline for Electron Storage," Energy Procedia 79, (2015): 903-909. https://doi.org/10.1016/j.egypro.2015.11.585

[9] P. N. Khanam, M. A. AlMaadeed. M. Ouederni, E. Harkin-Jones, B. Mayoral, A. Hamilton and D. Sun, "Melt Processing and Properties of Linear Low-Density Polyethylene-Graphene Nanoplatelet Composites," Vacuum 130 (2016): 63-71. https://dx.doi.org/10.1016/j.vacuum.2016.04.022

[10] M. Mehrali, E. Sadeghinezhad, S.T. Latibari, S.N. Kazi, M. Mehrali, M.N.B. Mohd Zubir and H.S.C. Metselaar, "Investigation of Thermal Conductivity and Rheological Properties of Nanofluids Containing Graphene Nanoplatelets," Nanoscale Research Letters 9, no. 15 (2014): 1-12. https://doi.org/10.1186/1556-276X-9-15

[11] Y. Sun and G. Shi, "Graphene/Polymer Composites for Energy Applications," Journal of Polymer Science, Part B: Polymer Physics 51, no. 4 (2012): 231-253. https://doi.org/10.1002/polb.23226

[12] T. Rajyalakshmi, A. Pasha, S. Khasim, M. Lakshmi and M. Imran, "Synthesis, Characterization and Hall-Effect Studies of Highly Conductive Polyaniline/Graphene Nanocomposites," SN Applied Sciences 2, no. 530 (2020): 1-11. https://doi.org/10.1007/s42452-020-2349-4

[13] M. Roudjane, M. Khalil, A. Miled and Y. Messaddeq, "New Generation Wearable Antenna Based on Multimaterial Fiber for Wireless Communication and Real-Time Breath Detection," Photonics 5, no. 4 (2018): 1-20. https://doi.org/10.3390/photonics5040033

[14] S. Khasim, "Polyaniline-Graphene Nanoplatelet Composite Films with Improved Conductivity for High Performance X-Band Microwave Shielding Application," Results in Physics 12, (2019): 1073-1081. https://doi.org/10.1016/j.rinp.2018.12.087

[15] N. Badi, S. Khasim and A.S. Roy, "Micro-Raman Spectroscopy and Effective Conductivity Studies of Graphene Nanoplatelets/Polyaniline Composites," Journal of Materials Science: Materials in Electronics 27, (2016): 6249-6257.
https://doi.org/10.1007/s10854-016-4556-8

[16] K. M.Molapo, P. M. Ndangili, R. F. Ajayi, G. Mbambisa, S.M. Mailu, N. Njomo, M. Masikini, P. Baker and E.I. Iwuoha,"Electronics of Conjugated Polymers (I): Polyaniline," International Journal of Electrochemical Science 7, (2012): 11859-11875.

[17] Y-S. Jun, J.G. Um, G. Jiang and A. Yu, "A Study on the Effects of Graphene Nano-platelets (GnPs) Sheet Sizes from a Few to Hundred Microns on the Thermal, Mechanical, and Electrical Properties of Polypropylene (PP)/GnPs Composites," eXPRESS Polymer Letters 12, no.10 (2018): 885-897.
https://doi.org/10.3144/expresspolymerlett.2018.76

[18] S.Y. Chin, T.K. Abdullah and M. Mariatti, "One-steps Synthesis of Conductive Graphene/Polyaniline Nanocomposites using Sodium Dodecyl Benzene Sulfonate: Preparation and Properties," Journal of Material Science - Materials Electronics 28 (2017): 18418-18428.
https://doi.org/10.1007/s10854-017-7788-3

[19] H. H. Shi and H.E. Naguib, "Fabrication and Characterization of Polyaniline-Graphene Nanoplatelets Composite Electrode Materials for Hybrid Supercapacitor Applications," SPIE Proceedings – Behaviour and Mechanics of Multifunctional Materials and Composites 9432, (2015): 94320U.
https://doi.org/10.1117/12.2083934

[20] A.Z. Elsherbani and M.J. Inman, "Antenna Design and Radiation Pattern Visualization," Applied Computational Electromagnetics Society Journal – Special Issues on ACES 2003 Conference – Part 1 18, no. 4 (2003): 26-32.

[21] Y. Ranga, K.P. Esselle and A.R. Weily," Compact Ultra-Wideband CPW-FED Printed Semicircular Slot Antenna," Microwave Optic Technology Letters 52, no. 10 (2010): 2367-2372.
https://doi.org/10.1002/mop.25481

[22] N. Singh, A. K. Singh and V. K Singh, "Design & Performance of Wearable Ultra Wide Band Textile Antenna for Medical Applications," De Gruyter Open Engineering 5, no.1 (2015): 117-123.
https://doi.org/10.1515/eng-2015-0012

[23] M. I. Shueb, M. E. Abd Manaf, C. T. Ratnam, N. Mohamad and M. Mohamed, "Enhancement of Mechanical and Electrical Properties in Graphene Nanoplatelet Modified Nylon 66," Malaysian Journal on Composite Science and Manufacturing 1, no. 1 (2020): 1-10.
https://doi.org/10.37934/mjcsm.1.1.110